Do Multilayer Crystals Nucleate in Suspensions of Colloidal Rods?

Alessandro Patti and Marjolein Dijkstra

Soft Condensed Matter, Debye Institute for NanoMaterials Science, Utrecht University, Princetonplein 5, 3584 CC Utrecht, The Netherlands

(Received 22 October 2008; published 24 March 2009)

We study the isotropic-to-crystal transformation in a mixture of colloidal hard rods and nonadsorbing polymer using computer simulations. We determine the height of the nucleation barrier and find that the critical cluster consists of a single crystalline layer growing laterally for all polymer fugacities considered. At lower supersaturation, the free energy of a single hexagonally packed layer increases monotonically with size, while the nucleation barrier of a second crystalline layer is extremely high. Hence, the nucleation of multilayer crystals is never observed. Multilayer crystals form only in the spinodal decomposition regime, either where, in an intermediate stage, single crystalline membranes coalesce into multilayer clusters or where, at higher polymer fugacity, smaller clusters of rods stack on top of each other to form long filaments. Eventually, these transient structures evolve into a thermodynamically stable bulk crystal phase.

DOI: 10.1103/PhysRevLett.102.128301 PACS numbers: 82.70.Dd, 68.55.A−, 82.60.Nh

It is well known that liquids must be supercooled substantially before they start to crystallize spontaneously, as the system has to cross a free energy barrier. If the free energy barrier is high, spontaneous fluctuations that would result in the formation of the stable phase are rare, and subcritical clusters that are formed will dissolve spontaneously. When spherical particles nucleate, the clusters that form tend to be spherical: e.g., gas bubbles in a superheated liquid, liquid droplets in a supersaturated gas, or roughly spherical crystallites in an undercooled liquid are undisputed transient clusters. On the other hand, nonspherical particles giving rise to liquid crystalline phases with positional and orientation ordering may form anisotropic clusters. The formation of the nematic phase which possess only orientational order is well-studied experimentally [1,2], by theory and simulations [3,4], and proceeds via the formation of spindle-shaped elongated nematic droplets, called tactoids. This state of affairs should be contrasted with the formation of clusters, where both orientation and positional order play a role. Simple transient smectic or crystalline droplets of anisotropic particles have to the best of our knowledge never been observed in experiments [1,5] or in simulations [6,7]. For instance, a simulation study on crystal nucleation in fluids of short hard rods shows that the growth of a single crystalline membrane is hampered by rods that are aligned parallel to the bottom and top surfaces of the crystallite: the surface poisons itself and hence prevents its own growth [6]. Another simulation study shows that the nucleation of the smectic phase in fluids of longer rods is hampered due to slow dynamics [7]. In this Letter, we study the interplay between orientation and positional order on the nucleation of anisotropic particles, where cluster formation is not inhibited by kinetic effects.

To this end, we study a mixture of hard rods and nonadsorbing polymer. The addition of polymer induces an effective attraction between the rods due to the so-called depletion attraction [8]. The range and strength of the attraction are determined by the diameter of the polymer coils and the polymer fugacity. Our model consists of hard spherocylinders (HSCs) with a length-to-diameter ratio of $L^* = L/D = 5$ and nonadsorbing ideal polymer with radius of gyration $R_g = D/4$. The presence of the polymer is described by an empiric effective depletion potential, which depends on the relative positions and orientations of the two rods, and is maximal for parallel and adjacent rods [8]. The addition of nonadsorbing polymer broadens the coexistence regions, yielding broad gas-crystal coexistence at sufficiently high polymer fugacity $z^* \equiv zD^3 > 2$ (see [8]). This allows us to study nucleation of clusters with positional and orientation order in a supersaturated dilute gas phase, where it is unlikely that the nucleation is hindered by self-poisoning or slow dynamics.

We study the isotropic-to-solid (IX) transition using Monte Carlo simulations in the isothermal-isobaric (*NPT*) ensemble. We perform simulations of 864 rods in a rectangular simulation box with periodic boundary conditions, and the length of the box sides are allowed to fluctuate. When the pressure $P^* = \beta P D^3$, with $\beta = 1/k_B T$, is slightly higher than the coexistence pressure, we employ the umbrella sampling technique to study the IX transformation [9]. We use the cluster criterion described in Ref. [4] to study crystal nucleation at a polymer fugacity $z^* > 3.0$, which lies inside a broad gas-solid coexistence region. For $3.0 < z^* < 3.9$, we observe nucleation and growth (NG) at low and spinodal decomposition (SD) at high supersaturation. For $z^* > 4.0$ (stronger attractions), we find SD for all supersaturations that we studied. In the NG regime, we calculate the Gibbs free energy ΔG as a function of cluster size by using umbrella sampling. In contrast with Ref. [6], where it was found that ΔG grows monotonically with cluster size and never crosses a barrier, we find a Gibbs free energy barrier for different pressures and polymer fugacities. In Fig. 1, we show the Gibbs free

energy barriers for $z^* = 3.0$ and various pressures. At this fugacity, the system exhibits a transition at $P^* = 0.002$ from an isotropic gas phase with density $\rho_I^* = ND^3/V = 0.0021$ to a dense solid phase with density $\rho_X^* = 0.154$. Exemplarily, we find for $P^* = 0.0205$ that the height of the nucleation barrier is $\Delta G^c \simeq 12 k_B T$ and the corresponding size of the critical crystal nucleus is $n^c = 28$, while for $P^* = 0.012$ (see inset) we find $\Delta G^c \simeq 87 k_B T$ and $n^c = 315$. Surprisingly, we find that the clusters that are formed consist of a single hexagonally ordered layer of rods that can grow spontaneously when the cluster exceeds the critical cluster size. However, these clusters grow only laterally; i.e., particles attach from the metastable isotropic fluid phase only on the edge of the growing cluster. Hence, we never observe the nucleation of additional layers and the formation of multilayer crystallites in our simulations. A typical configuration of such monolayers is shown in Fig. 1.

For $P^* > 0.0205$ (corresponding to $\Delta\mu^* > 2.23$, with $\Delta\mu^*$ the difference in chemical potential between the isotropic fluid phase and the crystal phase in units of $k_B T$), the nucleation barrier is very low, and we observe spontaneous NG of monolayer crystals without applying a biasing potential. The actual nucleation pathway is shown in the supplementary movie [10]. For $P^* < 0.012$ ($\Delta\mu^* < 1.74$), we find that the free energy grows monotonically with cluster size, and hence the system never crosses a nucleation barrier beyond which the cluster can grow spontaneously. Our simulations show that the growth of these clusters proceeds again via a monolayer and that the formation of multilayer crystals seems to be inhibited even if we bias the cluster size distribution to larger crystallites. The inhibition of the formation of multilayer clusters has also been observed in systems of pure hard rods and was attributed to kinetic reasons, e.g., self-poisoning or slow dynamics [6,7]. As in the present case the metastable isotropic fluid phase is extremely dilute, it is hard to envision that the nucleation of additional layers is hampered here by kinetic effects.

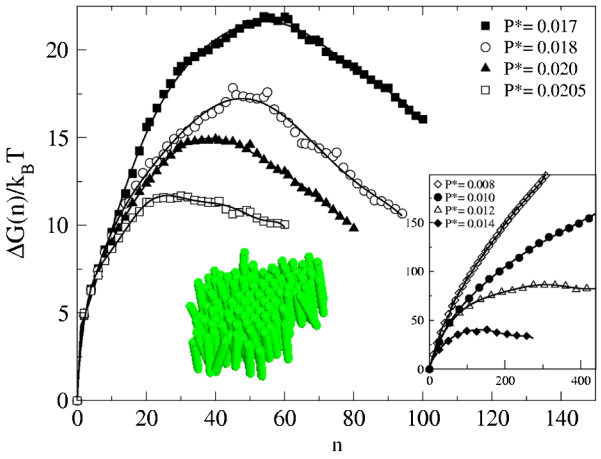

FIG. 1 (color online). Gibbs free energy ΔG as a function of the number of particles n in the biggest cluster for a mixture of HSCs with $L/D = 5$ and nonadsorbing polymer with $R_g = D/4$, polymer fugacity $z^* = 3.0$, and for $P^* = 0.017$, 0.018, 0.020, and 0.0205. The inset shows $\Delta G(n)$ for $P^* = 0.008$, 0.010, 0.012, and 0.014 (note the different scale). The lines are guides to the eye. A typical configuration of critical cluster is shown as the inset.

We compare our results for the nucleation barriers with the theoretical model for the growth of smectic or crystalline filaments in suspensions of colloidal rods [11]. In this work, the free energy associated with the formation of a single circular crystalline layer with radius R and height H is approximated to be

$$\Delta G = -\pi R^2 \rho H |\Delta\mu| + 2\pi R^2 \gamma_\perp + 2\pi R H \gamma_\parallel, \qquad (1)$$

with $\gamma_\perp$ and $\gamma_\parallel$ the interfacial free energy of the interface between the top and the edges of the crystalline layer and the isotropic phase, respectively. At low supersaturation $|\Delta\mu| < 2\gamma_\perp/\rho H$, ΔG is always positive, and consequently a single layer can never grow spontaneously. The free energy ΔG can become negative only by increasing the gain in bulk free energy compared to the interfacial free energy cost, and, hence, only multilayer crystals may grow spontaneously [11].

We fit our free energy barriers with Eq. (1) using $\gamma_\parallel$ and $\gamma_\perp$ as fitting parameters. In Fig. 2, we plot the simulation data along with the fits, and we find remarkably good agreement for all of our free energy curves if we use $\gamma_\parallel^* = 0.235$ and $\gamma_\perp^* = 0.803$, with $\gamma^* \equiv \beta\gamma D^2$. Note that the Gibbs free energies are plotted as a function of the radius R of the biggest cluster by employing $n = \pi\rho H R^2$. Using this value for $\gamma_\perp$, we find that the theory predicts a crossover at $|\Delta\mu| = 2\gamma_\perp/\rho H \simeq 1.738 k_B T$, which agrees surprisingly well with our simulation results: we observe a maximum in ΔG for $|\Delta\mu|^* \geq 1.74$ ($P^* \geq 0.012$), beyond

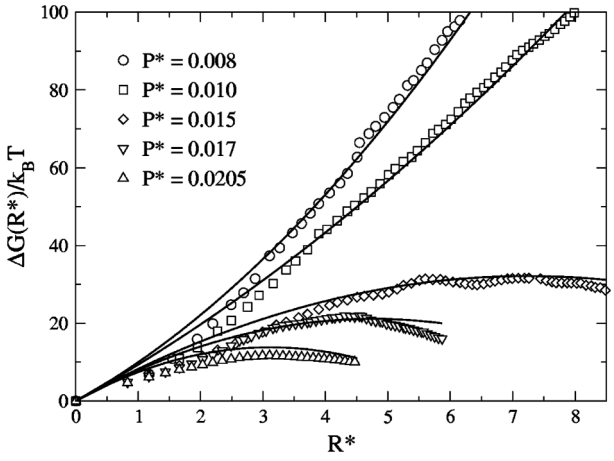

FIG. 2. Fits according to Eq. (1) to the Gibbs free energy curves displayed in Fig. 1, as a function of the radius $R^* = R/D$ of the cluster. The open symbols are simulation data at the pressures indicated. For clarity, we do not show the data for all of the pressures.

which a single membrane can grow spontaneously, while for $|\Delta\mu|^* \leq 1.57$ ($P^* \leq 0.010$) the monolayer cannot grow as ΔG increases monotonically with n.

We study the nucleation of a second layer on the first layer, as for $P^* < 0.012$ only multilayer crystals may grow spontaneously. Above, we mentioned that the growth of clusters proceeds via a single crystalline layer that grows only laterally even if we bias the cluster size distribution to larger crystallites. In order to prevent the growth of the first layer, we equilibrate an infinite monolayer consisting of 650 rods in a periodic box at $P^* = 0.010$ ($\Delta\mu^* = 1.57$) and $z^* = 3.0$. By applying the same umbrella sampling technique as employed above for the nucleation of the first layer, i.e., without any orientational bias as employed in Ref. [6], we observe the formation of a second layer on top of the monolayer, and we even find a nucleation barrier. In Fig. 3, we present the Gibbs free energy both for the formation of the first layer as well as for the second layer. Figure 3 shows clearly that a monolayer of size n has a lower free energy than a double layer of the same size when the second layer is subcritical. This explains why the monolayer grows only laterally when we bias the sampling towards larger cluster sizes. Moreover, we find that the free energy barrier for the second layer is extremely high, i.e., $\Delta G^c \simeq 90 k_B T$ for a second layer of size $n^c = 190$. If we assume that the second layer can be nucleated only on top of a monolayer with at least the same size and that the Gibbs free energy of a monolayer of size $n = 190$ is $\Delta G \simeq 90 k_B T$, we find that the probability to find a bilayer of this size is extremely small, i.e., $P(n = 380) \simeq \exp(-180)$. In conclusion, although the system should actually form the thermodynamically stable crystal phase, the nucleation of a postcritical cluster is extremely rare.

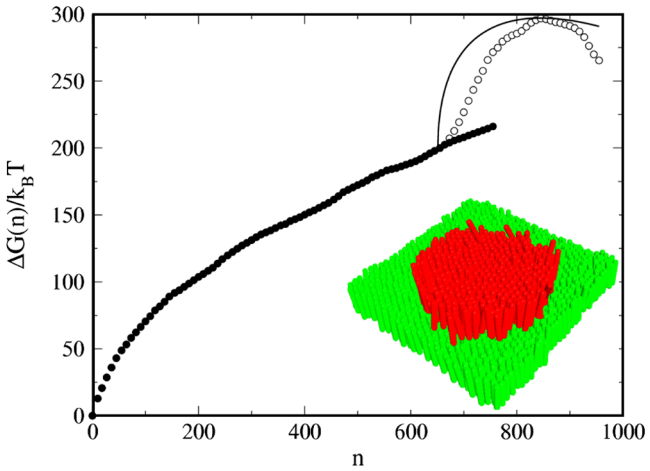

FIG. 3 (color online). Gibbs free energy ΔG as a function of the number of rods n of a monolayer (solid circles) and a double-layer crystal (open circles), at $z^* = 3.0$ and $P^* = 0.010$. The inset shows a typical configuration of 950 rods, where a second layer of 300 rods has been grown on top of an infinite layer. The solid line denotes the fit to the nucleation barrier of the second layer.

As our nucleation barriers for the monolayers are well described by Ref. [11], we can test our results for the second layer against this theory. The theoretical model predicts that the free energy to grow a second circular layer with radius R and height H is given by $\Delta G_2 = -\pi R^2 \rho H |\Delta\mu| + 2\pi R H \gamma_{\|}$, which assumes that the surface free energy for the top and bottom surfaces of the second circular layer cancels as we do not create an extra top surface. This expression would predict at $\Delta\mu^* = 1.57$ ($P^* = 0.010$) a critical cluster radius $R^c = \gamma_{\|}/(\rho|\Delta\mu|) \sim 1$, corresponding to a critical nucleus of about 3 rods, and a barrier height $\Delta G_2^c \sim 6 k_B T$. Here we use $\gamma_{\|}^* = 0.235$, which was already obtained from our fits in Fig. 2. The theory underestimates significantly the nucleation barrier and the critical nucleus size. This discrepancy can be caused only by a strong underestimation of the surface free energy cost of the second layer, as only an increase in free energy cost can increase the nucleation barrier. The missing contribution to the surface free energy cost can be resolved, if we consider the first layer as a substrate for the second layer. In that case, we can use Turnbull's extension of classical nucleation theory (CNT) to heterogeneous nucleation of a crystal on a wall [12], and then the Gibbs free energy is given by $\Delta G_2 = -\pi R^2 \rho H |\Delta\mu| + \pi R^2 (\gamma_{wx} - \gamma_{wi}) + \pi R^2 \gamma_{\perp} + 2\pi R (H\gamma_{\|} + \tau)$, where γ_{wx} and γ_{wi} denote the wall-crystal and wall-isotropic fluid interfacial tensions, respectively. In addition, we introduce a contribution to the free energy due to a line tension τ, as it was shown in Ref. [13] that the line tension cannot be neglected for wall-induced crystal nucleation in the case of hard spheres. We also set γ_{wi} equal to $\gamma_{\perp}$ as the wall-isotropic fluid interfacial tension should be (nearly) equal to the interfacial tension between the crystal and the isotropic fluid. Consequently, the Gibbs free energy reduces to $\Delta G_2 = -\pi R^2 \rho H |\Delta\mu| + \pi R^2 \gamma_{wx} + 2\pi R (H\gamma_{\|} + \tau)$. The nucleation barrier of the second layer is fitted with this equation using γ_{wx} and τ as fitting parameters. The fit is shown in Fig. 3 using $\gamma_{wx}^* = 0.984$ and $\tau = 2.408 k_B T/D$. We can reproduce a nucleation barrier with a barrier height similar to that in our simulations, but the shape of the free energy curve is poorly described. This discrepancy may be due to the fact that strong finite size corrections to the Gibbs free energy are expected for monolayer clusters, which should be investigated in future work. Indeed, recent simulations show evidence for large finite size effects in the surface free energy of NaCl crystallites, which was attributed to the faceted shape of the cluster [14].

As we find only nucleation of monolayers and the nucleation of additional layers is very unlikely, it is interesting to investigate how the stable crystal phase consisting of multiple crystalline layers will actually form. To study the formation of multilayer clusters, we study the system at higher supersaturations, where we observe spinodal decomposition. At low polymer fugacity, e.g., $z^* = 3.5$, we find that only a few clusters are formed at the beginning of the simulation, which tend to grow laterally as in the NG

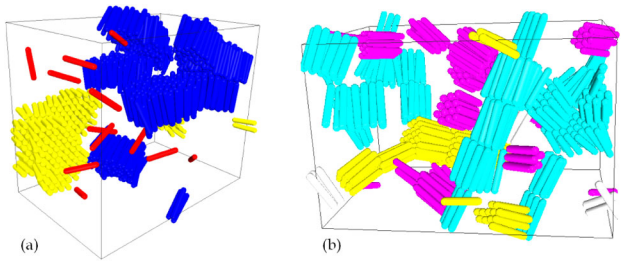

FIG. 4 (color online). Intermediate structures observed in the spinodal decomposition regime during the IX transformation. (a) Crystalline membranes observed at $z^* = 3.5$ and $P^* = 0.010$. (b) Smectic filaments at $z^* = 6.5$ and $P^* = 0.018$.

regime. Subsequently, at an intermediate stage of the phase transformation, the clusters, which grow to a considerable size, coalesce when they are close enough to each other. The coalescence can give rise to bigger membranes as they merge sideways, but occasionally, two monolayers form a bilayer by top-bottom coalescence. In Fig. 4(a), we show a typical example where two monolayers are about to merge into a bilayer. The actual pathway is shown in the supplementary movie [10]. Finally, the system evolves into a thermodynamically stable bulk crystal phase. At higher fugacities, i.e., $z^* = 6.5$ (stronger attractions), we find that the number of clusters that are formed at the beginning of the simulations is much higher than at lower fugacity, especially if the supersaturation is low. These clusters pile on top of each other and form relatively long filaments consisting of many different layers with a nonuniform thickness; i.e., each layer contains a different number of rods (see [10] for a movie). In an intermediate stage, the filaments form a percolating network, which eventually should evolve into the thermodynamically stable crystal phase. However, due to the strong attraction between the rods as the polymer fugacity is very high, a nonequilibrium gel-like structure is formed due to an arrested spinodal decomposition. Hence, we were not able to observe the equilibrium configuration within our simulations. Upon decreasing z^*, the thickness of the filaments increases and their length decreases, and hence the shape of the clusters can be tuned from monolayers to long and thin filaments. Our results agree with the experimental observations of Dogic and Fraden, who studied the kinetics of the isotropic-smectic transition in mixtures of rodlike viruses and nonadsorbing polymers [1]. In this work, long thin filaments are observed at high polymer concentrations and big freely floating monolayers, which can coalesce sideways and top-bottom at low z^*. The different structures can be explained by the depletion attraction between the rods and between the surfaces of two clusters. At high polymer fugacity, many clusters are formed immediately as the depletion attraction between the rods is very high. These clusters will quickly coalesce as the attraction of the clusters is also very high. At lower z^*, only a few clusters will be formed in the beginning, which will grow laterally because the attraction of two adjacent rods is higher than two rods head to tail. For sufficiently big clusters, the area of the top surface is sufficiently large and hence also the attraction, so that two clusters can merge top-bottom.

In conclusion, we have studied crystal nucleation of clusters with positional and orientation order in a dilute isotropic gas phase, where it is unlikely that the nucleation is hindered by kinetic effects. We observed that (i) only single crystalline layers can nucleate and grow as the nucleation of multilayer clusters is extremely rare, (ii) structures consisting of multiple layers can form only in the SD regime by top-bottom coalescence of single membranes, and (iii) the simulated nucleation barriers for monolayers are well described by the theoretical predictions of Ref. [11], while the nucleation barrier for the second layer is reasonably described by CNT for heterogeneous nucleation. In addition, our findings are in agreement with experimental observations in attractive β-FeOOH rod suspensions where matlike 2D clusters are formed that subsequently merge into 3D smectic structures [5] and with experiments on fd-virus particles where huge single monolayers are formed that form multilayer structures by top-bottom coalescence [1].

We thank A. Cuetos and E. Sanz for useful discussions. This work was financed by the NWO-VICI grant.

[1] Z. Dogic and S. Fraden, Phil. Trans. R. Soc. A **359**, 997 (2001); Z. Dogic, Phys. Rev. Lett. **91**, 165701 (2003).
[2] J. Viamontes *et al.*, Phys. Rev. Lett. **97**, 118103 (2006); Z. X. Zhang and J. S. van Duijneveldt, J. Chem. Phys. **124**, 154910 (2006); M. P. Lettinga *et al.*, J. Phys. Condens. Matter **17**, S3609 (2005); M. P. B. van Bruggen *et al.*, Macromolecules **32**, 2256 (1999).
[3] P. Prinsen and P. van der Schoot, Phys. Rev. E **68**, 021701 (2003).
[4] A. Cuetos and M. Dijkstra, Phys. Rev. Lett. **98**, 095701 (2007); A. Cuetos *et al.*, Soft Matter **4**, 757 (2008).
[5] H. Maeda and Y. Maeda, Phys. Rev. Lett. **90**, 018303 (2003).
[6] T. Schilling and D. Frenkel, Phys. Rev. Lett. **92**, 085505 (2004).
[7] A. Cuetos *et al.* (to be published).
[8] S. V. Savenko and M. Dijkstra, J. Chem. Phys. **124**, 234902 (2006).
[9] P. R. ten Wolde and D. Frenkel, J. Chem. Phys. **109**, 9901 (1998).
[10] See EPAPS Document No. E-PRLTAO-102-070914 for supplementary videos. For more information on EPAPS, see http://www.aip.org/pubservs/epaps.html.
[11] D. Frenkel and T. Schilling, Phys. Rev. E **66**, 041606 (2002).
[12] D. Turnbull, J. Chem. Phys. **18**, 198 (1950).
[13] S. Auer and D. Frenkel, Phys. Rev. Lett. **91**, 015703 (2003).
[14] T. Zykova-Timan *et al.*, Phys. Rev. Lett. **100**, 036103 (2008).